Design of switching sequences for sine parameters estimation on switched antenna arrays

Pierre Avital, Gilles Chardon, José Picheral

Design of switching sequences for sine parameters estimation on switched antenna arrays

Pierre Avital[a,b], Gilles Chardon[b], José Picheral[b]

firstname.lastname@centralesupelec.fr

[a] *Valeo CDA, 94000, Créteil, France*
[b] *Université Paris-Saclay, CNRS, CentraleSupélec, Laboratoire des signaux et systèmes, 91190, Gif-sur-Yvette, France.*

Abstract

Most research on source localization using arrays of antennas relies on the assumption that the array's antennas are all sampled at the same times. However, for RF signals, and especially in embedded systems, this is a very costly assumption to uphold.

In this paper, we consider the case where the antennas of the array are sampled by a single receiver channel, through the use of a switch. The main advantage of such a system is to reduce costs, but on the other hand, the samples are not measured at the same time on each antenna.

This paper deals with the design of the switching sequence that can dramatically impact the performance of sine parameters estimation in applications such as source localization.

Cramér-Rao Bounds (CRB) are computed in order to derive design criteria. From their analytic expression, guidelines are proposed in order to define switching sequences that provide good performances. In addition, numerical results allow to compare the performance of the proposed sequences to relevant lower bounds and to the performance of sequences obtained by an exhaustive search.

Keywords: Cramer-Rao Bounds, Array Signal Processing, Switched Array, Single Receiver, Source Localization.

Notations

- Indexing into a matrix or vector will be done using $[\cdot]_{i,j}$.
- Labeled variables are considered to belong to sets, and $\bar{\cdot}$ is used as a recursive centroid operator:
  Example: Let $\xi = \{\xi_a, \forall a \in [1, A]\}$, where $\xi_a = \{\xi_{a,b} \in \mathbb{R}, \forall b \in [1, B]\}$. The $\bar{\cdot}$ operator can be used on the individual sets ξ_a such that $\overline{\xi_a} = \frac{1}{B}\sum_{b=1}^{B} \xi_{a,b}$, or on the set ξ of these sets: $\overline{\xi} = \frac{1}{A}\sum_{a=1}^{A} \overline{\xi_a}$.

1. Introduction

Array signal processing has been a long-standing interest in signal processing, with applications such as Direction of Arrival (DOA) estimation [1], RADAR, imaging, etc. The most conventional methods for array signal processing, illustrated in Figure 1a, usually rely on matching each antenna with a receiver channel and an Analog-Digital Converter (ADC). The main advantage of this architecture is to provide simultaneous samples of the measured signal by each antenna.

However, for radio frequency (RF) applications for instance, receiver channels and their synchronization can be rather costly in many ways: most obviously financially, but also in terms of space for components, as well as energy consumption. These costs are especially an issue for embedded systems that may be strongly constrained in terms of energy and volume.

To mitigate these costs, a trending approach is to use a single receiver channel to sample all antennas, adding an electronic switch to select from which antenna each sample is taken, as illustrated in Figure 1b. This approach allows the removal of all receiver channel hardware chains (bandpass filter, superheterodyne, ADC...) but one; while an electronic switch and controling hardware must be added.

Since the signals measured on each antenna are not sampled simultaneously anymore, the design of such systems requires choosing a switching sequence in order to define when each antenna is sampled. An example of a signal received observed through such a system is illustrated in Figure 2.

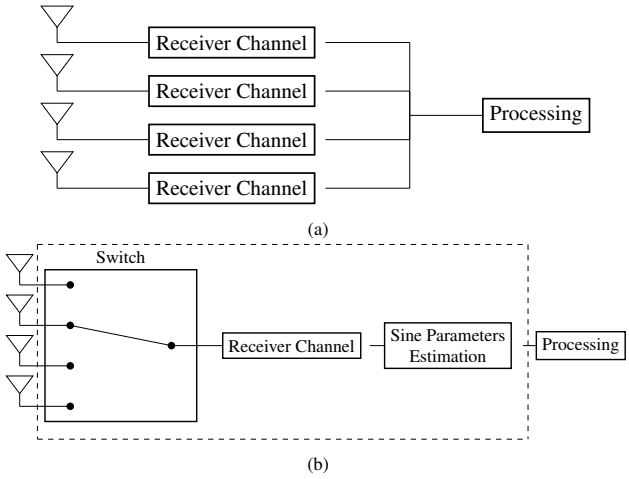

Figure 1: Examples of two systems for sampling and processing of the signals received by an array of antenna. On the left is the most classical system, associating a receiver channel to each antenna. On the right is the subject of this paper, where all antennas are sampled by a single receiver channel through a switch.

Earlier applications of switched antenna arrays to DOA estimation were proposed in [2] and [3], based on a beamformer network, and consists in measuring the signal power for several sets of beamforming weights in order to estimate the array covariance matrix. In [4], this method is generalized to a number of receiver channels larger than one, but smaller than the number of antennas, using a time-varying preprocessing.

In [5] and [6], DOA estimation using a sequential switching is considered (the switch is toggling from one antenna to the next between every sample). This allows the use of classical auto-covariance based algorithms such as MUSIC, with only a slight modification to the steering vectors employed. Nevertheless, this approach necessitates the use of costly high speed switches. To alleviate this issue, [6] also proposes using larger blocks, switching to each antenna only once. Blocks of multiple samples are also used in [7].

Switched arrays can also be used in active arrays, such as Frequency-Modulated Continuous Wave (FMCW) RADAR. In this context, signals are usually sampled in blocks corresponding to a pair of transmitting and receiving antennas. The case of linear arrays, with a unique transmitter, is considered in [8]. Robust estimation in the context of switched array FMCW RADAR is introduced in [9]. Automotive applications are developed in [10] and [11], where the influence of the order in which the antennas are switched on the estimation of the performances of the estimation is investigated. Cramér-Rao bounds for the estimation of the direction, velocity and range of targets are given in [12]. Calibration of fully-switched MIMO arrays is considered in [13].

In this paper, we assume that the signals we measure can be modeled as combinations of sinusoids in the interval where they are sampled. We will focus on the optimization of switching sequences for the classical problem of the estimation of their parameters (angular frequencys, amplitudes, and phases). While this problem arises in a large variety of applications, we consider here the case of passive DOA estimation using Bluetooth signals [14]. This context will guide our investigations, and provide the numerical values of the parameters used in the simulations. However, our conclusions remain relevant in wider contexts.

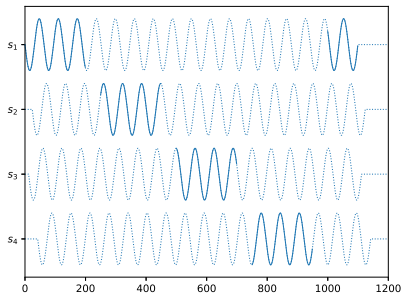

Figure 2: Example of switching strategies: solid lines are the signals sampled by the ADC.

The originality of this paper is to take into account hardware constraints in order to design switching sequences. The main constraint is that switching from one antenna to the other introduces a delay that causes a loss of samples. It is a well-known problem that is mentioned in the Constant Tone Extension (CTE) Bluetooth specification [15] for Bluetooth 5.1. Obviously, sample loss can be avoided by the use of costly high speed switches, but this solution is generally discarded since the main goal of using a single received channel antenna is to reduce the hardware costs.

Additionally, in this paper, we assume that the frequencies of each source are unknown or poorly known and must be estimated. For example, the Bluetooth specification allows for a deviation of up to ±75kHz around the nominal center frequency, making said nominal frequency a worse guess than a frequency estimation when working with a decent signal-to-noise ratio (SNR), as will be shown later. We justify the need for frequency estimation by the two following points:

- In DOA estimation problems, the frequency is part of the parameters used to compute the array manifold, implying that significant errors in the frequency will lead to errors in the array manifold. However, this issue is small for most applications, as the tolerated deviation of a center frequency is typically much smaller than the center frequency itself, by at least 5 orders of magnitude in Bluetooth's case.

- As the signals received by the antennas are not sampled simultaneously, an accurate estimation of the frequency is necessary to estimate phase differences between two signals. Indeed, the phases of the signal have to be estimated at a common point in time, at which at most one signal is measured. Any mismatch between the actual frequency of the signals and its estimation will lead to a proportional error in phases estimation. As an example, an error of 50kHz on the center frequency is allowed by the Bluetooth specification, yet offsets the measured phase by 5% of a turn

every microsecond away from the time reference (i.e., at each sample with a sampling rate of 1 MHz). While it is a non-issue for K-antenna-K-channel systems, as the signals are acquired simultaneously, it can be non-negligible for switched systems where the samples associated to two different antennas can be separated by a time delay such that the phase error introduced by the frequency mismatch is larger than the error introduced by measurement noise by one or more orders of magnitude at decent SNR.

To our knowledge, there is no work in the literature which deals with the issue of designing a switching sequence for sinusoidal parameter estimation in the case of a single receiver channel. We will show that the choice of switching sequence impacts dramatically the performance of the frequency and phase estimates as it will be illustrated in section 3.

The main contribution of this paper is to provide tools to optimize the switching sequence. In other words, we answer to the question: "when and which antenna must be sampled by the unique ADC in order to get the most accurate estimation of the parameters of a sinusoidal model".

The method proposed to optimize switching sequence is the following: first, the Cramér-Rao Bound (CRB) matrix is derived for the model parameters; secondly, using the CRB matrix, scalar *design criteria* are defined for the amplitudes, angular frequency, and phases estimation respectively. The analytic expressions of these criteria allow us to provide some basic rules to design smart switching strategies. Finally, strategies are proposed and compared to theoretical lower bounds as well as the criteria for the best sequence resulting of a quasi-exhaustive search.

This paper will follow this structure: the data model is introduced in Section 2, a preliminary example is proposed in Section 3 in order to motivate this work. In Section 4, the Cramér-Rao Lower Bounds (CRB) are derived and in Section 5 the design criteria are proposed. In Section 6 several ways of building smart switching sequences are discussed, and the numerical results of Section 7 allow us to compare the performance of the proposed switching sequences and to comment on the influence of some parameters. Finally, conclusions are drawn in Section 8.

2. Model

2.1. Signal model

Assuming that the signal measured on each antenna (labeled k) can be modeled as a sum of I complex exponential, the noise free model is given by:

$$s_k(t) = \sum_{i=1}^{I} A_{i,k} \mathrm{e}^{\mathrm{j}\phi_{i,k}} \exp(\mathrm{j}\omega_i t), \tag{1}$$

where $\omega_i \in \mathbb{R}$, $A_{i,k} \in \mathbb{R}^+$ and $\phi_{i,k} \in [0, 2\pi]$ are the model parameters.

Let us show that the proposed model can be used to formulate multi-source, multipath DOA 2D localization problems, while not being restricted to this application. For this application, relevant notably to the automotive industry, each source is considered to emit pure sines at different frequencies, which are unknown or partially known to the receiver. Multipath propagation channels can affect the received signal.

The pure sinusoidal nature of each source's signal is justified by an effort of the embedded systems' industry to solve positioning problems, which has commonly resulted in means to emit pure sines, such as the Constant Tone Extension (CTE), added to the Bluetooth specification [15] in Bluetooth 5.1.

Consider a planar array of K antennas, labeled 1 through to K, where the k^{th} antenna has position $\zeta_k = (x_k, y_k)^T$, such that the array's centroid is $\frac{1}{K}\sum_{k=1}^{K} \zeta_k = (0,0)^T$, where $\cdot^T$ denotes transposing the vector.

Consider I sources, the i^{th} source emitting a sinusoidal signal with an angular frequency ω_i. Due to a multipath propagation channel, for each source, L_i reflections are impinging on the antenna array, the l^{th} path of the i^{th} source's signal is characterized by its direction of arrival ($\alpha_{i,l}$) and complex amplitude ($\beta_{i,l}$).

For each path, we also define the time of arrival at the centroid of the array ($\tau^{(0)}_{i,l}$); and the propagation delay ($\tau_k(\alpha_{i,l})$) between the centroid of the array and the k^{th} antenna. Assuming that the sources are in far-field and that the signals propagates at a celerity of c, the delay at the k^{th} antenna $\tau_k(\alpha)$ can be expressed as a function of the direction of arrival α:

$$\tau_k(\alpha) = \frac{1}{c}\zeta_k^T \cdot \begin{pmatrix}\cos\alpha \\ \sin\alpha\end{pmatrix}. \tag{2}$$

We can then write the noise-free received signal as follows:

$$s_k(t) = \sum_{i=1}^{I}\sum_{l=1}^{L_i} \beta_{i,l} \exp(\mathrm{j}\omega_i(t - \tau_k(\alpha_{i,l}) - \tau^{(0)}_{i,l})). \tag{3}$$

Eq (3) can indeed be rewritten as the proposed model in eq (1) where the complex magnitudes $A_{i,k}\mathrm{e}^{\mathrm{j}\phi_{i,k}}$ carry the information for direction of arrival estimation and are written as:

$$A_{i,k}\mathrm{e}^{\mathrm{j}\phi_{i,k}} = \sum_{l=1}^{L_i} \beta_{i,l} \exp(\mathrm{j}\omega_i(\tau_k(\alpha_{i,l}) + \tau^{(0)}_{i,l})), \tag{4}$$

In the following of this paper, we will focus on the bounds of the variance of the estimates of ω_i, $A_{i,k}$ and $\phi_{i,k}$. Indeed, these parameters can be used to compute DOA estimations (as eq (4) forms a system of equations that may be used to solve for $\alpha_{i,l}$), but they have the advantage that they don't require assuming the geometry of the antenna network.

2.2. Measurement model

The key difference between more common systems (where each antenna is sampled simultaneously by a corresponding receiver channel) and the single receiver channel system is that, in the second case, the system has to switch from one antenna to the other in order to measure samples. As a result, in the first case, all the antenna are sampled at the same instants, while in the second case, the sampling instants differ for each antenna to the next. Let's introduce a notation that allows us to reason about sampling instants.

Assuming that N_k samples are measured at the output of the k^{th} antenna, let $\mathcal{T}_k = \{t_{k,n}, \forall n \in [1, N_k]\}$ be the set of the N_k sampling instants, where $t_{k,n}$ is the sampling instant of the n^{th} samples of the k^{th} antenna. Similarly, let $x_{k,n}$ be the n^{th} sample measured at the output of the k^{th} antenna, it can be written as:

$$x_{k,n} = s_k(t_{k,n}) + \varepsilon_{k,n}, \tag{5}$$

where $\varepsilon_{k,n}$ is an additive complex noise supposed to be spatially and temporally white with variance σ^2.

Although this paper mainly focuses on the case of a single receiver channel, this model, as well as the bounds and criteria derived from it, aren't restricted to this case. All the expressions from sections 2, 4 and 5 are applicable to any system which samples the signal of the K antennas through K or less receiver channels. They are therefore applicable to subarray sampling techniques, as proposed by [16] and developped upon by [17].

3. Preliminary example

We present here some simulation results in order to motivate the work presented in this paper aiming at optimizing the choice of switching sequences. As we will see below, the performances are significantly impacted by the switching sequence.

To illustrate this fact, a simple example has been chosen: consider only one source assuming that the noise is Gaussian, measurements are performed with a four elements antenna array with a switch fast enough such that no samples are lost during the switching. For the sake of simplicity, we focus only on frequency estimation (but, as shown in the following section, a poor accuracy of the frequency estimate also degrades the phase estimates).

Performance are evaluated using the Maximum Likelihood Estimator (MLE). In this case (only one source with gaussian noise), it is well known that the MLE criterion can be computed by a Discrete-Time Fourier Transform (DTFT) defined by:

$$\tilde{x}(\nu) = \frac{1}{K} \sum_{k=1}^{K} \left| \sum_{n=1}^{N_k} x_{k,n} \exp\left(-\mathrm{j}2\pi\nu \frac{t_{k,n}}{T}\right) \right|^2. \tag{6}$$

The following parameters are used in the simulation: $K = 4$ antennas, sampling period is $T = 1$, source angular frequency is $\omega_1 = 0.2\pi$ which corresponds to a normalized frequency $\nu_1 = 0.1$, the number of samples $N_k = 32$ is the same for each antenna and Signal to Noise Ratio (SNR) is set to 10 dB.

For this example, we consider only basic sequences which sequentially switch to the next antenna, the difference between the sequences is the number of samples which are measured on each antenna between each switching. These sequences are illustrated in Figure 3. The MLE criteria associated to the following switching sequences are plotted in Figure 4:

1. Measuring one sample and then switching to the next antenna: it requires $N-1$ switching operations (i.e., a switching for each sample).
2. Measuring N_k samples and then switching to the next antenna: it requires only $K-1$ switching operations (i.e., a single samples block per antenna).
3. Measuring $\frac{N_k}{2}$ samples and then switching to the next antenna: it requires $2K-1$ switching operations (i.e., two samples blocks per antenna).

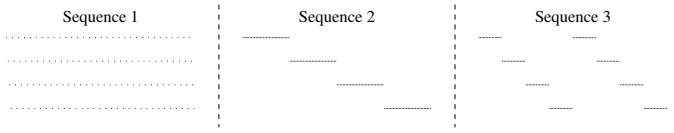

Figure 3: Switching sequences used in this example, each dot represents a sample. Horizontal axis is time. Each vertical levels corresponds to one of the four channels.

Note that while sampling all samples from a single antenna would yield better frequency estimation than any of these other techniques, it would also make phase estimation impossible for the other antennas without either taking several measurements, or an additional receiver channel; both cases not being considered by paper.

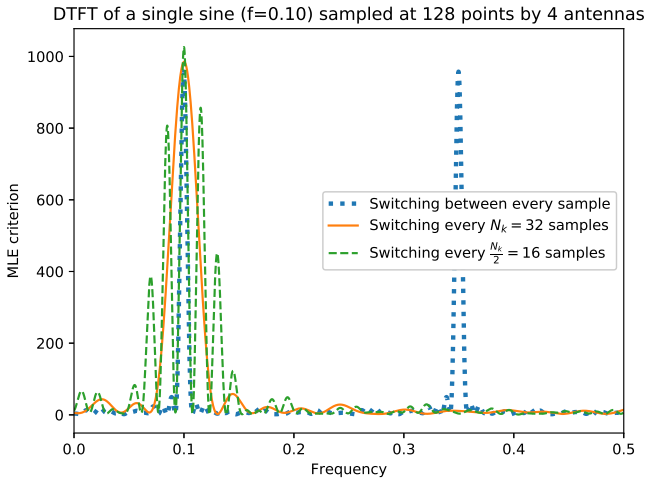

Figure 4: Comparison of the MLE criterion for angular frequency estimation with three sampling strategies.

The performance of the estimator is mainly impacted by aliasing and the width of the peak (spectral resolution). From Figure 4, one can notice that these three sequences provide criteria with different features:

- Switching between each sample provides a narrow peak, but causes spectrum aliasing. The aliasing is due to the fact that the effective sampling rate on each antenna is divided by the number of antennas.
- Switching between each block of N_k samples solves the issue of spectrum aliasing, but the peak is wider. The poor frequency resolution is due to the reduction of the length of the observation window (in this case: $N_k T$ instead of $K N_k T$)
- The in-between method of switching twice to each antenna provides a much narrower peak, while avoiding the issue of spectrum aliasing. It does however display greater side

lobes, due to the rather unconventional window function this sampling equates to.

This example illustrates that the switching strategy can dramatically influence the performances of the estimators. It motivates our work to optimize the switching strategy in order to provide the best performance for angular frequency and phase estimation.

4. Cramér-Rao bounds

As a first step towards the design of sampling schemes, CRBs are computed for the estimation of the amplitudes and phases, and when applicable, angular frequency, of multiple sinusoidal signals of identical frequency.

CRBs give a lower bound on the covariance matrix of an unbiased estimator $\hat{\boldsymbol{\theta}}$ of a vector of parameters $\boldsymbol{\theta}$, in the sense that the covariance matrix $\boldsymbol{\Sigma}_{\hat{\boldsymbol{\theta}}}$ of $\hat{\boldsymbol{\theta}}$ is necessarily larger (in the Loewner order of semi-positive definite matrices) than the matrix $\mathbf{CRB}$, obtained as the inverse of the Fisher Information Matrix (FIM). In particular, the variances of the estimation of the parameters are bounded from below by the diagonal coefficients of the matrix $\mathbf{CRB}$.

In general, coefficients of the FIM $\mathbf{F}$ are given by the expectation of the second derivative of the log-likelihood function with respect to the parameters.

In the particular case where measurements are modeled as a complex random gaussian vector with mean $\mathbf{s}(\boldsymbol{\theta})$ and constant covariance matrix $\boldsymbol{\Sigma}_{\boldsymbol{\epsilon}}$, the coefficients of $\mathbf{F}$ can be found using the simpler Slepian-Bangs formula [18, 19, 20]

$$[\mathbf{F}]_{i,j} = 2\mathrm{Re}\left(\frac{\partial \mathbf{s}^H}{\partial [\boldsymbol{\theta}]_i} \boldsymbol{\Sigma}_{\boldsymbol{\epsilon}}{}^{-1} \frac{\partial \mathbf{s}}{\partial [\boldsymbol{\theta}]_j}\right). \tag{7}$$

A further simplification can be made when the measurement noise is white, as the coefficients $[\mathbf{F}]_{i,j}$ can be written as the sum of the Fisher information of each sample. In our case, with complex noise samples of variance $2\sigma^2$,

$$[\mathbf{F}]_{i,j} = \sum_{k=1}^{K} \sum_{n=1}^{N_k} [\mathbf{F}_{k,n}]_{i,j}\,, \tag{8}$$

where

$$[\mathbf{F}_{k,n}]_{i,j} = \frac{1}{\sigma^2}\mathrm{Re}\left(\frac{\partial s_{k,n}{}^{\star}}{\partial [\boldsymbol{\theta}]_i} \frac{\partial s_{k,n}}{\partial [\boldsymbol{\theta}]_j}\right). \tag{9}$$

The coefficients of the FIM in the case of multiple sources are given in appendix A. We will focus on the case of a unique source with

$$s_{k,n} = A_k e^{i\phi_k} e^{i\omega t_{kn}}, \tag{10}$$

where simple and interpretable bounds are found. We computed these CRBs in two cases:

- known angular frequency ω, with parameters $\boldsymbol{\theta} = (A_1, \ldots, A_K, \phi_1, \ldots, \phi_K)$,
- unknown angular frequency, with parameters $\boldsymbol{\theta}' = (A_1, \ldots, A_K, \omega, \phi_1, \ldots, \phi_K)$.

Quantities (e.g. FIM, CRBs, etc.) associated to the unknown angular frequency case will be identified by a prime symbol $(\cdot')$ when necessary.

4.1. Known angular frequency

A common assumption for DOA estimation is that the carrier angular frequency is known. Under this assumption the Fisher information matrix is diagonal:

$$\mathbf{F} = \begin{bmatrix} \mathbf{F}_A & 0 \\ 0 & \mathbf{F}_\phi \end{bmatrix} \tag{11}$$

where the diagonals of the $K \times K$ blocks $\mathbf{F}_A$ and $\mathbf{F}_\phi$ are

$$[\mathbf{F}_A]_{k,k} = N_k/\sigma^2 \tag{12}$$

$$\left[\mathbf{F}_\phi\right]_{k,k} = A_k^2 N_k/\sigma^2. \tag{13}$$

The CRB matrix as the same structure as $\mathbf{F}$, where its two diagonal blocks $\mathbf{CRB}_A$ and $\mathbf{CRB}_\phi$, have diagonal coefficients given by:

$$[\mathbf{CRB}_A]_{k,k} = \frac{\sigma^2}{N_k} \tag{14}$$

$$\left[\mathbf{CRB}_\phi\right]_{k,k} = \frac{\sigma^2}{A_k^2 N_k}. \tag{15}$$

4.2. Unknown angular frequency

As explained in the introduction, there are circumstances where a source may emit a signal with an angular frequency significantly different from the nominal one, hence the need to estimate the angular frequency ω of the received signal.

In this case, the FIM takes the following shape:

$$\mathbf{F}' = \begin{bmatrix} \mathbf{F}_A & 0 & \mathbf{0} \\ 0 & \mathrm{F}_\omega & \mathbf{f}_{\omega,\phi}^{\star} \\ \mathbf{0} & \mathbf{f}_{\omega,\phi} & \mathbf{F}_\phi \end{bmatrix} \tag{16}$$

with $\mathbf{F}_A$ as in (12), $\mathbf{F}_\phi$ as in (13), and

$$\mathbf{F}_\omega = \sum_{k=1}^{K} A_k^2 \sum_{n=1}^{N_k} t_{kn}^2/\sigma^2 \tag{17}$$

$$\left[\mathbf{f}_{\omega,\phi}\right]_k = A_k^2 \sum_{n=1}^{N_k} t_{kn}/\sigma^2 \tag{18}$$

Owing to the diagonal block structure of $\mathbf{F}'$, CRBs for the estimates of A_1 through A_K remain the same as in eq (14), and the CRB matrix $\mathbf{CRB}'$ is structured as

$$\mathbf{CRB}' = \begin{bmatrix} \mathbf{CRB}_A & 0 & \mathbf{0} \\ 0 & \mathrm{CRB}_\omega & \mathbf{crb}_{\omega,\phi}^{\star} \\ \mathbf{0} & \mathbf{crb}_{\omega,\phi} & \mathbf{CRB}_\phi' \end{bmatrix}. \tag{19}$$

After inversion of the remaining block associated to the angular frequency and the phases (e.g. applying Cramer's rule), the bounds related to the angular frequency ω is

$$\mathrm{CRB}_\omega = \frac{\sigma^2}{\sum_{k=1}^{K} A_k^2 N_k \Lambda_k}, \tag{20}$$

where $\Lambda_k = \frac{1}{N_k}\sum_{n=1}^{N_k}(t_{k,n} - \overline{t_k})^2$ is the dispersion of the sampling instants of the k^{th} antenna.

The block $\mathbf{CRB}'_\phi$ related to the phases $(\phi_1, \ldots, \phi_K)$ has coefficients

$$\left[\mathbf{CRB}'_\phi\right]_{i,j} = \delta_{i,j}\frac{\sigma^2}{A_i^2 N_i} + \mathrm{CRB}_\omega \overline{t_i}\,\overline{t_j} \tag{21}$$

where $\delta_{i,j}$ is the Kronecker symbol, and

$$\left[\mathbf{crb}_{\omega,\phi}\right]_k = -\mathrm{CRB}_\omega \overline{t_k}. \tag{22}$$

We note that, compared to the previous case, an additional term appears in $\mathbf{CRB}'_\phi$, due to the estimation error of the angular frequency ω. This additional term is positive in the diagonal, confirming the expected fact that phase estimation errors are higher when the angular frequency is unknown.

4.3. Cyclic bounds

One can note that the parameters ϕ_k are 2π periodic and ω is $2\pi f_s$. The provided CRBs bound the variance of unbiased estimators, but they don't take their periodicity into account.

Since the periodic estimates are bounded, the estimation error is bounded for low SNR, and the CRB cannot be considered anymore in such regimes.

To take the estimator's periodicity into account, [21] proposes to measure the error of an estimator using the Mean Cyclic Error (MCE) instead of the MSE, the latter being equivalent to the estimator's variance when the estimator is unbiased:

$$\mathrm{MCE}_{\phi_k\in[0,2\pi]} = E\left[\left|1 - \mathrm{e}^{\mathrm{j}\left(\widehat{\phi_k}-\phi_k\right)}\right|^2\right], \tag{23}$$

[21] then shows that a bound on the MCE can be derived from a bound on the MSE. Namely, $\mathrm{CRB}^{\mathrm{cyc}}_{\phi_k\in[0,2\pi]}$ can be derived from CRB_{ϕ_k}

$$\mathrm{CRB}^{\mathrm{cyc}}_{\phi_k\in[0,2\pi]} = 2 - 2(1 + \mathrm{CRB}_{\phi_k})^{-\frac{1}{2}} \tag{24}$$

To keep the MCE's useful properties of being a lower bound for the MSE and converging with it for smaller values, even when the estimator's period $\nu \neq 2\pi$, the following expression of the MCE may be used for the angular frequency estimator:

$$\mathrm{MCE}_{\omega\in[0,2\pi f_s]} = f_s^2 E\left[\left|1 - \mathrm{e}^{\mathrm{j}\frac{\widehat{\omega}-\omega}{f_s}}\right|^2\right], \tag{25}$$

This expression of the MCE is then bound by:

$$\mathrm{CRB}^{\mathrm{cyc}}_{\omega\in[0,2\pi f_s]} = 2f_s^2 - 2f_s^2\left(1 + \frac{\mathrm{CRB}_\omega}{f_s^2}\right)^{-\frac{1}{2}}. \tag{26}$$

Note that the cyclic and non-cyclic bounds converge for lower values, as do the MSE and MCE.

4.4. Numerical validation

To validate the analytical expressions of the CRBs, Monte-Carlo simulations were used to estimate the MSE and MCE of the Maximum Likelihood Estimator, and compare them with the corresponding CRBs and cyclic CRBs.

The MLE is defined by $\widehat{\theta'} = \underset{\theta'}{\mathrm{argmax}}\; l(x|\theta', \sigma)$ where $l(x|\theta', \sigma)$ is the log-likelihood of the measured signal x, and in our case is written:

$$l(x|\theta', \sigma) = \sum_{k=1}^{K}\sum_{n=1}^{N_k}\left(-\log(2\pi\sigma^2) - \frac{1}{2\sigma^2}\left|x_{k,n} - s_{k,n}(\theta')\right|^2\right). \tag{27}$$

During simulations, the parameters were estimated using gradient descent, with an initial parameters vector θ'_0 computed by a Discrete Fourier Transform (equivalent to a grid search of the MLE).

The simulations were run with various SNRs, with a reference θ' corresponding to physical parameters relevant to our application (Bluetooth Low Energy): a signal with $f = 2.4$GHz, impinging from $\theta = \pi$ on a circular array of $K = 4$ antennas and radius $r = 0.5$m, sampled at $N = 160$ points with sample rate $f_s = 1$MHz, switching antenna instantly ($D = 0$) between each sample. 10000 trials were used to estimate the performances.

The results of these simulations are displayed on Figures 5 and 6, where the MSE, MCE and corresponding CRBs are ploted with respect to the SNR, for frequency and phase estimation respectively.

As can be observed on Figures 5 and 6, the MCE and MSE converge with both the periodic and aperiodic bounds in the asymptotic low-noise regime [22].

Tighter bounds could be obtained in low SNR regimes, for example with Barankin bounds ([23]). However, our application domain (source localization over Bluetooth communications) tends to guarantee high SNR (15dB being required for a better than 0.1% Binary Error Rate ([24, 25]), which is the highest allowed in Bluetooth before packet rejection), such that these bound aren't necessary.

Note from Figure 5 that for this lowest acceptable SNR of 15dB, the standard deviation on frequency estimation is of less than 10Hz. Thus, estimating the frequency yields a much better estimate of its value than the nominal value, which tolerates a discrepancy of up to ±75kHz.

Since the aperiodic bounds allow analytical simplifications, and converge with the periodic ones where they are relevant to our application, we will keep using the aperiodic bounds for the rest of this paper.

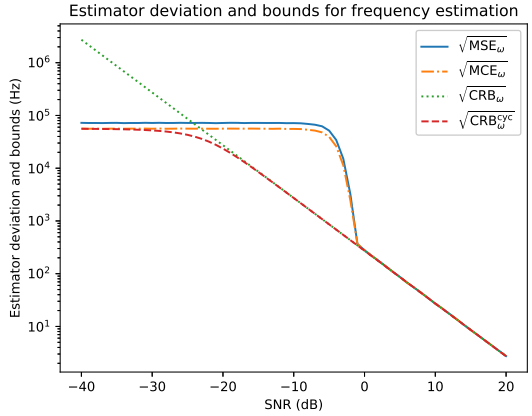

Figure 5: Estimator deviation and bounds for frequency estimation.

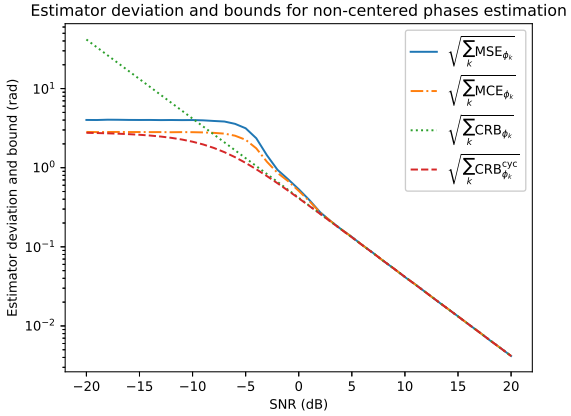

Figure 6: Estimator deviation and bounds for phases estimation.

5. Design criteria

In a multivariate setting, CRBs cannot be readily used to compare sampling designs. Indeed, it is not always possible to compare the CRBs of two different designs, as the Loewner order is not total.

5.1. Criteria definition

Following the approach of optimal design of experiments (in particular, A-optimal designs) [26], we will use three scalar criteria Γ_ω, Γ_A, and Γ_ϕ, related to the angular frequency, amplitudes, and phases respectively.

The criterion for the angular frequency is simply its CRB:

$$\Gamma_\omega = \mathrm{CRB}_\omega. \tag{28}$$

For the amplitudes, we define Γ_A as the sum of the CRBs of the amplitudes at each antenna (or, equivalently up to a multiplicative constant, their mean):

$$\Gamma_A = \sum_{k=1}^{K} [\mathbf{CRB}_A]_{k,k} \tag{29}$$

$$= \sum_{k=1}^{K} \frac{\sigma^2}{N_k}. \tag{30}$$

Using the same type of criterion for the phases yields in the known angular frequency case

$$\sum_{k=1}^{K} \left[\mathbf{CRB}_\phi\right]_{k,k} = \frac{\sigma^2}{A_k^2 N_k}, \tag{31}$$

and in the unknown angular frequency case

$$\sum_{k=1}^{K} \left[\mathbf{CRB}'_\phi\right]_{k,k} = \sum_{k=1}^{K} \frac{\sigma^2}{A_k^2 N_k} + \mathrm{CRB}_\omega \sum_{k=1}^{K} (\overline{t_k})^2. \tag{32}$$

In the latter case, this first criterion cannot be used to rank sampling designs. Indeed, shifting the time axis (which is equivalent to applying a constant phase shift over all antennas) should not influence the estimation error of direction of arrival, as the model is time invariant, whereas (32) is affected by such a shift. Likewise, the criterion should not take into account phase estimation errors common to all antennas.

For a better characterization of the performances of a switching strategie, we consider the centered estimators

$$\widehat{\phi}_k^c = \widehat{\phi}_k - \overline{\widehat{\phi}}, \tag{33}$$

obtained by removing the average of the estimation of the phases. This modification has no effect on the estimation of directions of arrival, and thus its variance. The sum of the variances of the estimated phases can be decomposed as

$$\sum_{k=1}^{K} \mathrm{var}\left(\widehat{\phi}_k\right) = \sum_{k=1}^{K} \mathrm{var}\left(\widehat{\phi}_k^c\right) + K\mathrm{var}\left(\overline{\widehat{\phi}}\right), \tag{34}$$

where the second term has no influence on the DOA estimation error.

We propose to define Γ_ϕ as a lower bound of the first component $\sum_{k=1}^{K} \mathrm{var}\left(\widehat{\phi}_k^c\right)$. The estimators $\widehat{\phi}_k^c$ can be written as $\widehat{\phi}_k^c = \mathbf{m}_k \widehat{\boldsymbol{\phi}}$, where $[\mathbf{m}_k]_{i\in[1,K]} = \delta_{i,k} - \frac{1}{K}$ and $\widehat{\boldsymbol{\phi}}$ is the vector of the estimates $\widehat{\phi}_k$. The variance of the centered estimators are $\mathrm{var}\left(\widehat{\phi}_k^c\right) = \mathbf{m}_k \boldsymbol{\Sigma}_\phi \mathbf{m}_k{}^*$, where $\boldsymbol{\Sigma}_\phi$ is the covariance matrix of $\widehat{\boldsymbol{\phi}}$. Moreover, as $\boldsymbol{\Sigma}_\phi$ and $\mathbf{CRB}_\phi$ are principal blocks of $\boldsymbol{\Sigma}_\theta$ and $\mathbf{CRB}$ respectively, $\boldsymbol{\Sigma}_\phi$ is bounded from below by $\mathbf{CRB}_\phi$ in the Loewner order. The variance of each centered estimator $\hat{\phi}_k^c$ can then be bounded by

$$\mathrm{var}\left(\widehat{\phi}_k^c\right) = \mathbf{m}_k \boldsymbol{\Sigma}_\phi \mathbf{m}_k{}^* \tag{35}$$

$$\geq \mathbf{m}_k \mathbf{CRB}_\phi \mathbf{m}_k{}^*. \tag{36}$$

Finally, the criterion for phases, in the known angular frequency case, is

$$\Gamma_\phi = \sum_{k=1}^{K} \mathbf{m}_k \, \mathbf{CRB}_\phi \, \mathbf{m}_k{}^* \tag{37}$$

$$= \frac{K-1}{K} \sum_{k=1}^{K} \frac{\sigma^2}{A_k^2 N_k}. \tag{38}$$

The same approach in the unknown angular frequency case yields the criterion

$$\Gamma'_\phi = \sum_{k=1}^{K} \mathbf{m}_k \, \mathbf{CRB}'_\phi \, \mathbf{m}_k{}^* \tag{39}$$

$$= \overbrace{\frac{K-1}{K} \sum_{k=1}^{K} \frac{\sigma^2}{A_k^2 N_k}}^{\Gamma_\phi} + \overbrace{\mathrm{CRB}_\omega \sum_{k=1}^{K} (\overline{t_k} - \bar{t})^2}^{\Gamma_2}. \tag{40}$$

We emphasize here the fact that Γ'_ϕ is time-invariant: replacing the sampling times t_{kn} by $t_{kn}+\delta$ for an arbitrary shift δ leaves Γ'_ϕ constant.

5.2. Interpretation of the criteria

Using the criteria defined above, properties of efficient sampling designs can be outlined. For the sake of simplicity, we will assume the amplitudes A_k are equal, as is the case of DOA estimation for far-field sources with a single path.

The criterion Γ_A, common to the known and unknown angular frequency cases, is minimized when the number of samples is similar on each antenna. Indeed, the relaxed minimization problem

$$\min_{z_k \in \mathbb{R}^+} \sum_{k=1}^{K} \frac{1}{z_k} \text{ such that } \sum_{k=1}^{K} z_n = N \tag{41}$$

has solution $z_k = N/K$. Minimization of Γ_ϕ is obtained under the same condition.

In the unknown angular frequency case, Γ_ω is minimized when the average dispersion $\overline{\Lambda}$ of the samples is maximized, implying that for each antenna, the samples should be spread the most possible. Finally, the criterion Γ'_ϕ is the sum of two terms Γ_ϕ and Γ_2. As above, minimizing the first term Γ_ϕ implies similar numbers of samples for each antenna. The second term is the product of the CRB of the angular frequency and the spread of the average of the sampling times on each antenna. Thus, the spread of the sampling instants should be maximized on each antenna, while concurrently the mean sampling times of the antennas should be similar.

5.3. Numerical validation

Monte-Carlo simultations were used (using the same parameters as in subsection 4.4) to validate the criteria discussed above.

On Figure 7, the RMSE of the MLE of the centered phases and its bound $\sqrt{\Gamma'_\phi}$. As expected, the RMSE converges to the bound for high SNR.

Since the estimates of ϕ are bounded (as discussed in subsection 4.3), the same applies to ϕ^c.

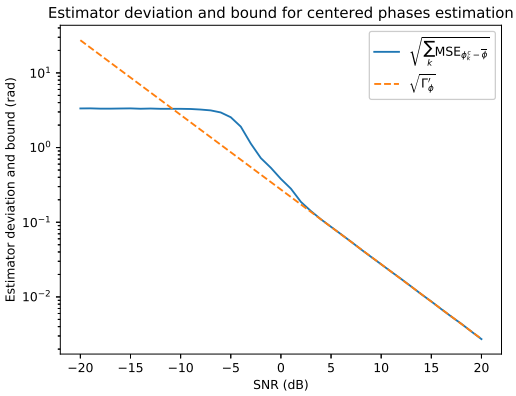

Figure 7: Deviation of the estimates of ϕ^c and corresponding bound $\sqrt{\Gamma'_\phi}$.

6. Switching sequences and strategies

In the previous section, Cramér-Rao bounds, as well as the bound Γ'_ϕ on the variances of the estimated centered phases, were given for arbitrary times $t_{k,n}$. Because Γ'_ϕ is non-convex in function of the sampling times, and because of the large number of variables, minimization of Γ'_ϕ is an intractable problem. In this section, using design constraints imposed by typical RF equipment, the complexity of the optimization problem is reduced.

6.1. Defining switching sequences

In order to restrict the search space for the optimization of the lower bound Γ'_ϕ, some assumptions are made on the switching sequences:

- for each antenna, sampling times are assumed to be drawn from an underlying regular sampling of the window of period T_s,
- at any given time, at most one antenna is active,
- switching between antennas implies a loss of D samples.

Under these assumptions, a switching sequence is characterized by its number M of blocks (that are defined as consecutive samples on a given antenna), their length L_m, and S_m, the index of the selected antenna in the m^{th} block. An example of such a description is given in figure 8.

The number of lost samples D is due to the switching delay that occurs when switching between antennas. Note that while $D = 0$ is possible (i.e. switching is guaranteed to have happened at the predicted time, and that signals have stabilized before the next sample), it requires the hardware to be able to reliably start switching between antennas after a given n^{th} sample and for the new signal to have stabilized before the next sample is to be taken. Doing so when working with radio-waves may require

specialized and costly hardware. We will assume that D is a constant associated with any given system.

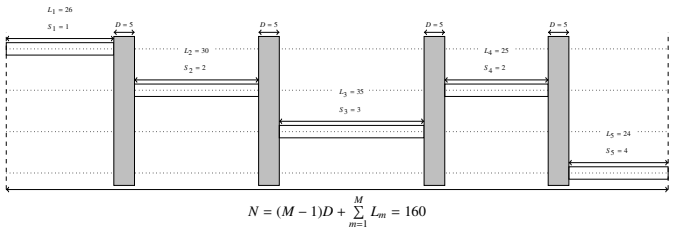

Figure 8: Example of a switching sequence

Still, even expressed as such, the search space for an optimal strategy is immense. To further reduce its dimension, we impose the additional constraint that all sampling blocks have the same size B, except for a unique block of length $r < B + D$, named "remainder block".

6.2. Simple sequences

The following sequences are the sequences we have found used either in other papers, or used within the industry, and are usually the result of applying intuition to the selection of a switching sequence.

6.2.1. Switching between each sample

One simple form of sampling would be switching between each sample, as done in [5] and [6]. As long as $D = 0$, this strategy provides good results, as the spread of the samples for a given antenna is large, and the mean sampling times for each antenna are close. However, in cases where $D > 0$, switching between each sample implies the loss of numerous samples, leaving approximately $N/(1 + D)$ samples available to estimate of the signal parameters instead of N.

An additional limitation of this sequence is the reduced range for the estimation of the angular frequency ω, as each antenna's sampling is decimated by a factor of $K(D + 1)$. This limitation can be mitigated by using a higher sampling rate and a proportionally faster switch, which comes at a higher cost.

6.2.2. One block per antenna

Opposite to switching between each sample, this strategy attempts to minimize the losses incurred by discarding $D > 0$ samples between each block: it reduces the number of blocks to the bare minimum: with $B = \left\lfloor \frac{N}{K} \right\rfloor$, only one block is used per antenna, obtaining the maximum total of $N - D(K - 1)$ samples, distributed as fairly as possible.

While this strategy minimizes Γ_ϕ (and is thus optimal when the angular frequency ω is known), its performances are degraded when the angular frequency ω has to be estimated. Indeed, with one block per antenna, the dispersion of the samples for each antenna is limited, which implies a large lower bound CRB_ω. Moreover, the dispersion of the mean sampling times for each antenna is large, yielding a large Γ_2 component for the bound Γ'_ϕ.

6.3. Exhaustive search

As the number of possible sequences under the above assumptions is finite for a given block size B, an exhaustive search for the best lower bound Γ_ϕ can be performed.

Every unique switching sequence possible with a given B was generated, for every position of the rest block; in the case where two consecutive blocks were assigned to the same antenna, the blocks were fused, including the D samples in between.

This way of exploring meant that for any given B, the search space for an optimal value of Γ_ϕ grows exponentially with regard to the maximum number of blocks that can be formed $M_{\max} = \left\lceil \frac{N}{B+D} \right\rceil$. This meant that we could only run combinatory searches within reasonable computing times for smaller values of $M_{\max}$.

6.4. Strategies

Since exhaustive search is not tractable for the smallest values of B, we propose two strategies to build switching sequences, as illustrated in Figure 9.

Two types of sequences are tested, with varying block size B.

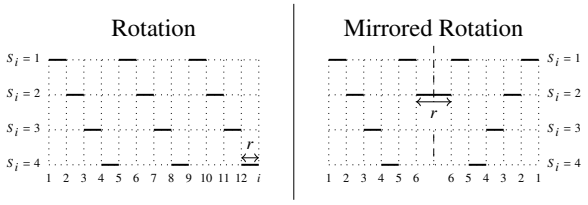

Figure 9: *Rotation* and *mirrored rotation* sequences, with 12 blocks for 4 antennas.

6.4.1. Rotation

The *Rotation* strategy switches from one antenna to the next every B samples, in a circular fashion. The sequence is described by $S_m = m \bmod K$ and $L_m = B$ (except for the last block of length r, which collects the remaining samples).

An advantage of this method is that the set of sampling times of the different antennas are related by a translation, which can be convenient for algorithms that rely on snapshots being taken with time axes that are translations of each other (such as ESPRIT or MUSIC [1]).

Remark: the simple sequences introduced in Section 6.2 may be generated by this strategy, with parameters $B = 1$ (6.2.1), or $M = K$ (6.2.2). All sequences used in the example provided in Section 3 may also be generated for $K = 4$ and $N = 128$ by the *Rotation* strategy with parameters $B = 1$, $B = 32$ and $B = 16$, respectively.

6.4.2. Mirrored Rotation

The *Mirrored Rotation* strategy applies the *Rotation* strategy to the first $\left\lceil \frac{N}{2} \right\rceil$ samples, followed by its reverse, as illustrated in Figure 9.

The symmetry of the sequence guarantees that the sample sets of each antenna share the same centroid nullifying the Γ_2 term in the lower bound Γ'_ϕ.

A limitation of this sequence, in particular compared to the Rotation sequence, is that sampling sets do not have the same shape for different antennas, which may complicate the task of forming snapshots for e.g. the application of the MUSIC algorithm.

7. Results

In this section, values of the criterion Γ_ω and Γ'_ϕ are discussed. Firstly, numerical values of the criteria are plotted in function of the block size for the strategies introduced in the above section, with fixed number of antennas K and window length N. Then, asymptotic values are given for large K and N.

7.1. Criteria in function of the block size

The simulation results presented in this section have been obtained with parameters values relevant to the application for the localization of Bluetooth Low Energy emitters. The number of antenna is $K = 4$, the source frequency is 2.4GHz, sampling rate is fixed to $f_s = 1$MHz, the total number of samples (included discarded samples) is $N = 160$, the number of discarded samples during each switching is $D = 3$. These parameters are derived from the CTE part of the Bluetooth specifications [15].

For simplicity, we assume that $A_i = A_j \; \forall i, j$. The SNR for all the following figures is 20 dB.

The Figure 10 shows the main optimization criterion Γ'_ϕ defined in eq (40) with respect to the block length (B) for the particular case where the switching follows a *Rotation* strategy as defined in section 6.

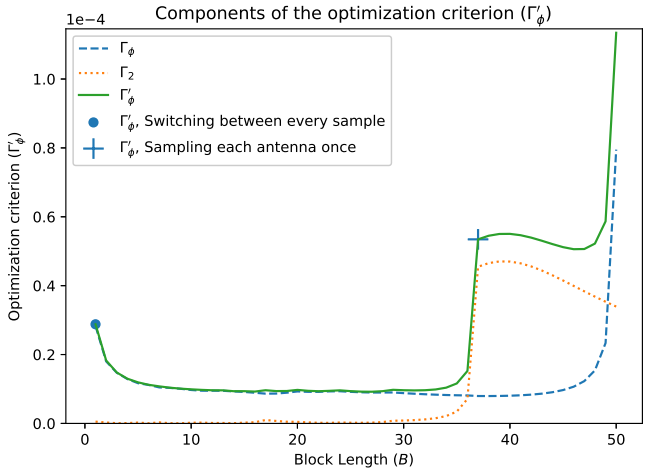

Figure 10: Optimization criterion $\Gamma'_\phi = \Gamma_\phi + \Gamma_2$ and its components against the block length B, using the *Rotation* strategy, with $K = 4$,$D = 3$ and $N = 160$.

This example shows that the block length can dramatically impact the performance of the estimator (remind that Γ'_ϕ is a lower bound of the sum of the variances of the estimated phases). In particular, the two simplest strategies (often proposed in the literature) are far from the optimal: switching between each sample (marker 'o') or switching only each antenna once (marker '+') increases respectively 3 or 6 times the criterion with respect to its lowest value. This remark motivates the search of optimal switching strategy.

In order to understand the behavior of the Γ'_ϕ curve, we analyze separately the two terms Γ_ϕ and Γ_2 of eq (40). First, one can notice that neither Γ_ϕ nor Γ_2 is negligible.

Let consider Γ_ϕ and remind that, from eq (38), it is minimized when the number of samples is maximal on each antenna and consequently:

- when the block length is small ($B \lesssim 10$), the number of blocks grows and with it, the number of samples discarded due to switching delays, which mostly increases Γ_ϕ,
- when the block length is too high ($B \gtrsim 48$), the number of samples for the last block is close to zero, causing a sharp increase of the variance of the phase in the last antenna, and of Γ_ϕ.

Focusing on Γ_2, from eq (40), it is clear that the minimization of this term requires that the centroids $\overline{t_k}$ of the sampling instants are the same for each antenna and/or that the average dispersion of sampling instants is large. The second conditions is verified when the block length is small enough ($B \lesssim 30$) so that at least one antenna has at least two separated blocks. Contrariwise, for $B \gtrsim 35$, the antennas are sampled by a unique block of limited dispersion, implying large values of Γ_2.

Coming back to Γ'_ϕ curve, one can note that a large range of value allows to roughly minimize the criterion ($20 \lesssim B \lesssim 30$). The exact value of B which minimizes Γ'_ϕ depends on the switching delay (and thus on D): obviously, when D increases, the number of switching must be reduced (and thus B should be greater). Empirically, we find that even with high values of D, at least $K + 1$ sampling blocks should be made in order to take advantage of the massive drop in Γ_2 caused by doing so.

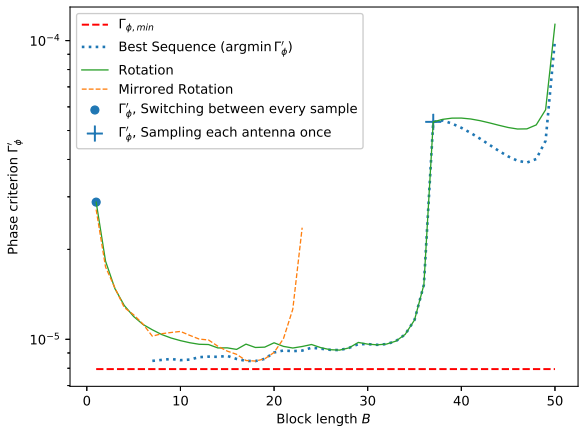

Figure 11: Phase criterion Γ'_ϕ against blocks length. Comparison of three strategies with equal blocks size: *Rotation*, *Mirrored Rotation* strategies and optimal sequence.

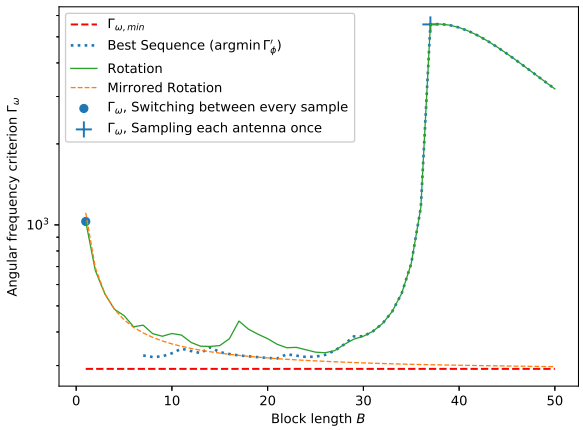

Figure 12: Angular frequency criterion Γ_ω against blocks length. Comparison of three strategies with equal blocks size: *Rotation*, *Mirrored Rotation* strategies and optimal sequence.

Figures 11 and 12 allow to compare the switching strategies presented in section 6. The lower bound $\Gamma_{\phi,\min}$ plotted for reference in Figure 11 is obtained by discarding the second term Γ_2, by assuming that $D = 0$ and that there are the same number of samples on each antenna ($N_1 = N_2 = \ldots = N_K = \frac{N}{K}$) such that:

$$\Gamma_{\phi,\min} = \frac{K-1}{N} \sum_{k=1}^{K} \frac{\sigma^2}{A_k^2}. \tag{42}$$

Similarly, in Figure 12, a lower bound $\Gamma_{\omega,\min}$ is obtained by considering the case where the signal would be sampled on a single antenna, discarding no samples:

$$\Gamma_{\omega,\min} = \frac{\sigma^2}{A_1^2 \sum_{n=1}^{N} \left(nT_s - \frac{(N+1)T_s}{2}\right)^2} \tag{43}$$

As pointed above, the simplest sequences (see Section 6.2) plotted with markers '+' and 'o' provide performances far from the optimal.

As expected, the exhaustive search among fixed block length sequences provides the best result and approaches the optimal lower bound. Both the rotation and mirrored strategies reach its performances for $25 \lesssim B \lesssim 38$ and $B \approx 20$ respectively.

7.2. DOA estimation

Addressing the specific issue of DOA estimation with a single receiver channel, one can wonder if the results established above are useful to design switching sequences in order to reduce DOA estimation errors.

To calculate the bounds on the DOA estimation errors, the antenna geometry must be taken into account, making it difficult to obtain generic results. In addition, analytical expressions of the bounds seem untractable.

For these reasons, we focus on numerical evaluation of these bounds, for a 20cm wide Uniform Linear Array (ULA) and a Uniform Circular Array (UCA) with a diameter of 20cm; each array being made of $K = 4$ antennas.

The FIM for DOA estimation in the single signal, single direction, case can be derived from eq (3) as shown in appendix C, and be numerically inverted to provide bounds for specific geometries that take the switching sequence into account.

Figures 13 and 14 allow us to compare the variations of the Γ'_ϕ criterion and CRB_α with respect to the bloc length B with the Rotation and Mirrored Rotation strategies.

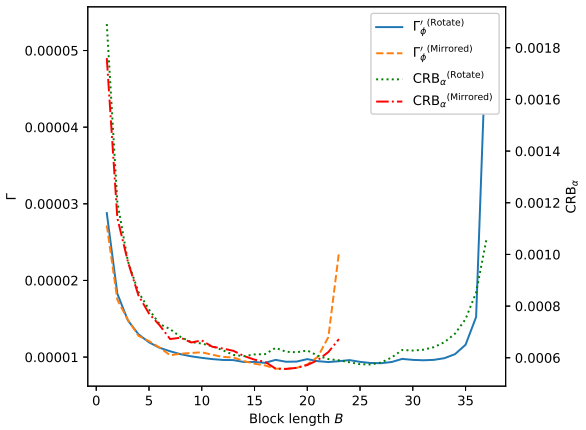

Figure 13: Phase criterion Γ'_ϕ and CRB_α against blocks length, for a $K = 4$ elements, 20cm diameter Uniform Circular Antenna.

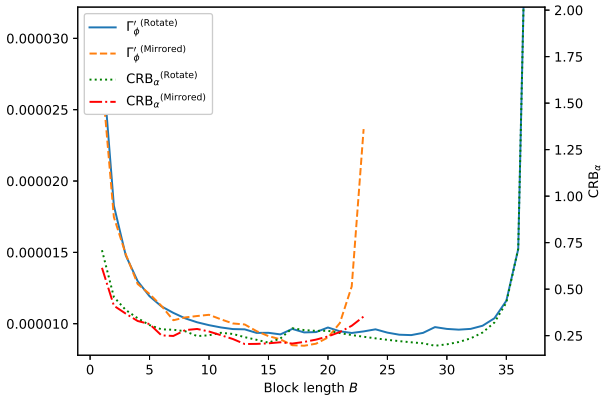

Figure 14: Phase criterion Γ'_ϕ and CRB_α against blocks length, for a $K = 4$ elements, 20cm wide Uniform Linear Antenna.

These figures illustrate that Γ'_ϕ varies similarly with the accuracy of DOA estimation, despite being computed with no knowledge of the array that the switching sequence would be used with.

Figure 14 does however show that when working with known array geometries, it may be wiser to compute the DOA bound directly (as provided in appendix C), as the Γ'_ϕ criterion will not *necessarily* have exactly the same minimum as the DOA estimation bound.

However, the DOA bounds for both the ULA and UCA match the Γ'_ϕ criterion with regard to how both of the simple switching sequences (switching between each sample and switching to each antenna exactly once) offer poor performances.

7.3. Asymptotic analysis of the criteria

Approximate values of the criteria are given on table 1 in the asymptotic regime for a large number of antennas K and a large window length N, using $D = 0$ and uniform amplitudes $A_k = A$. They are given for the rotation strategy with $M = K$ (one block for each antenna), $M = K + 1$ (the last block is allocated to the same antenna as the first one), and $M = 2K$ (each antenna is visited twice). Results are also given for the mirrored strategy where the second half of the rotation strategy with $M = 2K$ is reversed, and for a K receiver channels system which samples the signal for the same duration as the other systems, taking the same total number of samples.

Strategy	Parameters	Γ_A, Γ_ϕ	Γ_ω	Γ_2	Γ'_ϕ
Rotation	$M = K$	$\frac{K^2}{N}$	$\frac{12K^2}{N^3}$	$\frac{K^3}{N}$	$\frac{K^3}{N}$
Rotation	$M = K + 1$	$\frac{K^2}{N}$	$\frac{2K}{N^3}$	$\frac{K^2}{6N}$	$\frac{7}{6}\frac{K^2}{N}$
Rotation	$M = 2K$	$\frac{K^2}{N}$	$\frac{16}{N^3}$	$\frac{K}{3N}$	$\frac{K^2}{N}$
Mirrored Rotation	$M = 2K$	$\frac{K^2}{N}$	$\frac{12}{N^3}$	0	$\frac{K^2}{N}$
K channels	$N_k = N/K$	$\frac{K^2}{N}$	$\frac{12}{N^3}$	0	$\frac{K^2}{N}$

Table 1: Asymptotic values of the criteria with large number of antennas K and window length N. Actual values are obtained by multiplying Γ by σ^2, Γ_ϕ, Γ'_ϕ and Γ_2 by σ^2/A^2, and Γ_ω by $\sigma^2/(T_s^2 A^2)$. The "K channels" line corresponds to a system with one channel per antenna, taking $N_k = N/K$ synchronized samples per antenna over the same duration as the switched systems.

Firstly, notice that the Γ_A and Γ_ϕ, respectively the amplitude criterion and the phase criterion when the frequency is known, do not vary with respect to the sequence.

When each antenna is only visited once (Rotation, $M = K$), the frequency criterion Γ_ω scales with K^2, implying a large value for the Γ_2 term of Γ'_ϕ, the phase criterion when frequency is unknown.

Visiting the first antenna again at the end of the sequence (Rotation, $M = K + 1$) reduces Γ_ω by an order of magnitude in K, giving Γ_2 the same order as Γ_ϕ, thus making Γ'_ϕ the same order as Γ_ϕ, yet larger.

When each antenna is visited twice in identical order (Rotation, $M = 2K$), the bound Γ_ω is of the same order as the bound on frequency estimation with a single antenna. The Γ_2 term becomes of lower order than Γ_ϕ: Γ'_ϕ becomes of the same order as its known freqency equivalent Γ_ϕ.

Finally, Γ_ω is of exactly the order of single antenna frequency estimation both when visiting each antenna twice in opposite orders (Mirrored Rotation) and when sampling all antennas at the same times. In both cases, $\Gamma_2 = 0$ and $\Gamma'_\phi = \Gamma_\phi$.

With the last 3 sampling sets, Γ'_ϕ is either marginally or not affected by the necessity of estimating the frequency.

7.4. Discussion

Although the problem of finding the best switching sequence for the criteria defined above is not solved due to its combinatorial challenge, the numerical and asymptotic values of the criteria allow outlining some key features that switching sequences should have to allow good estimation performances.

Three key points are necessary to assure good performances:

- high dispersion of sampling instants must be guaranteed at least one antenna,
- the number of samples must be roughly the same for each antenna,
- the number of switching (or equivalently the number of blocks per antennas) should be limited to avoid discarding too many samples.

In any case, as discussed above, the number of blocks should be $K + 1$ or greater in order to provide a high instant sampling dispersion.

The mirrored strategy, for which Γ_2 is zero, exhibits performances that are not affected by the necessity to estimate the angular frequency, and was shown to be the best strategy in both numerical and asymptotic results.

Although its performances are slightly lower than the mirrored strategy, the *Rotation* strategy with $2K$ blocks has the advantage of having a simple structure. Indeed, the sampling times of each antenna are related by a time delay, allowing the use of subspace estimation methods such as MUSIC.

8. Conclusion

In this study, we aimed to improve the way arrays of antennas are sampled through a switch by a single receiver channel, as this type of setup is gaining popularity, especially in embedded RF solutions.

By computing the Cramér-Rao Bound, we have been able to propose readable analytic forms of design criteria to propose switching sequences. This analysis allows to give guidelines to attain better performances without hardware changes: switching sequences should distribute roughly the same number of samples between antennas and attempt to reduce the number of samples lost due to switching. In addition, when the angular frequency must be estimated, the dispersion of sampling instants must be maximized for at least one of the antennas, and each set of sampling instants should share the same centroid.

Strategies to define switching sequences have been proposed and compared to the simple sequences typically used in the previous works on switched arrays. Numerical results show that said sequences can provide poor performances, especially when estimating the angular frequency. The proposed *Mirrored Rotation* strategy reaches the performance of the sequence obtained by an exhaustive search; whereas the *Rotation* strategy with $M = 2K$ still provides good performances while being more convenient for classical algorithms such as MUSIC.

A. Fisher's Information Matrix

Although section 4 only shows the FIM for the case where the signal is a single sine, as only this case can be inverted analytically with legible results, the FIM $\mathbf{F}'$ for multiple sines of unknown frequencies with an AWGN of variance $2\sigma^2$ is still

writable as:

$$\mathbf{F}' = \begin{bmatrix} \mathbf{F}'^{(1,1)} & \mathbf{F}'^{(1,2)} & \dots & \mathbf{F}'^{(1,I)} \\ \mathbf{F}'^{(2,1)} & \mathbf{F}'^{(2,2)} & \dots & \mathbf{F}'^{(2,I)} \\ \vdots & \vdots & \ddots & \vdots \\ \mathbf{F}'^{(I,1)} & \mathbf{F}'^{(I,2)} & \dots & \mathbf{F}'^{(I,I)} \end{bmatrix} \tag{44}$$

with

$$\mathbf{F}'^{(i,j)} = \mathbf{F}'^{(j,i)^T} = \begin{bmatrix} \mathbf{F}_{A,A}^{(i,j)} & \mathbf{f}_{A,\omega}^{(i,j)} & \mathbf{F}_{A,\phi}^{(i,j)} \\ \mathbf{f}_{A,\omega}^{(i,j)^T} & f_{\omega,\omega}^{(i,j)} & \mathbf{f}_{\omega,\phi}^{(i,j)^T} \\ \mathbf{F}_{A,\phi}^{(i,j)^T} & \mathbf{f}_{\omega,\phi}^{(i,j)} & \mathbf{F}_{\phi,\phi}^{(i,j)} \end{bmatrix} \tag{45}$$

where $F'^{(i,j)}$ pertains to the i^{th} and j^{th} sources, $\mathbf{F}_{A,A}^{(i,j)}$, $\mathbf{F}_{\phi,\phi}^{(i,j)}$ and $\mathbf{F}_{A,\phi}^{(i,j)}$ are diagonal matrices, and $\mathbf{f}_{A,\omega}^{(i,j)}$ and $\mathbf{f}_{\omega,\phi}^{(i,j)}$ are column vectors such that:

$$\sigma^2 \left[\mathbf{F}_{A,A}^{(i,j)}\right]_{k,k} = \sum_{n=1}^{N_k} \cos(\Delta_{i,j,k,n}) \tag{46}$$

$$\sigma^2 \left[\mathbf{F}_{\phi,\phi}^{(i,j)}\right]_{k,k} = A_{i,k}A_{j,k} \sum_{n=1}^{N_k} \cos(\Delta_{i,j,k,n}) \tag{47}$$

$$\sigma^2 \left[\mathbf{F}_{A,\phi}^{(i,j)}\right]_{k,k} = -A_{j,k} \sum_{n=1}^{N_k} \sin(\Delta_{i,j,k,n}) \tag{48}$$

$$\sigma^2 f_{\omega,\omega}^{(i,j)} = \sum_{k=1}^{K} A_{i,k}A_{j,k} \sum_{n=1}^{N_k} t_{k,n}^2 \cos(\Delta_{i,j,k,n}) \tag{49}$$

$$\sigma^2 \left[\mathbf{f}_{A,\omega}^{(i,j)}\right]_k = -A_{j,k} \sum_{n=1}^{N_k} t_{k,n} \sin(\Delta_{i,j,k,n}) \tag{50}$$

$$\sigma^2 \left[\mathbf{f}_{\omega,\phi}^{(i,j)}\right]_k = A_{i,k}A_{j,k} \sum_{n=1}^{N_k} t_{k,n} \cos(\Delta_{i,j,k,n}) \tag{51}$$

$$\text{where } \Delta_{i,j,k,n} = (\omega_i - \omega_j)t_{k,n} + \phi_{i,k} - \phi_{j,k} \tag{52}$$

The FIM $\mathbf{F}$ for multiple sines of known frequencies under the same noise conditions can be similarly written:

$$\mathbf{F} = \begin{bmatrix} \mathbf{F}^{(1,1)} & \mathbf{F}^{(1,2)} & \dots & \mathbf{F}^{(1,I)} \\ \mathbf{F}^{(2,1)} & \mathbf{F}^{(2,2)} & \dots & \mathbf{F}^{(2,I)} \\ \vdots & \vdots & \ddots & \vdots \\ \mathbf{F}^{(I,1)} & \mathbf{F}^{(I,2)} & \dots & \mathbf{F}^{(I,I)} \end{bmatrix} \tag{53}$$

with

$$\mathbf{F}^{(i,j)} = \mathbf{F}^{(j,i)^T} = \begin{bmatrix} \mathbf{F}_{A,A}^{(i,j)} & \mathbf{F}_{A,\phi}^{(i,j)} \\ \mathbf{F}_{A,\phi}^{(i,j)^T} & \mathbf{F}_{\phi,\phi}^{(i,j)} \end{bmatrix} \tag{54}$$

Note that $\Delta_{i,i,k,n} = 0 \,\forall i,k,n$, leading to the simpler structure of the FIM for a single sine as used in section 4.

B. Inversion of the FIM

The block of the FIM $\mathbf{F}'$ related to the frequency ω and the phases ϕ has the shape of the following matrix $\mathbf{M}$:

$$M = \begin{bmatrix} a_0 & a_1 & a_2 & \cdots & a_K \\ a_1 & b_1 & 0 & \cdots & 0 \\ a_2 & 0 & b_2 & & 0 \\ \vdots & \vdots & & \ddots & \vdots \\ a_K & 0 & 0 & \cdots & b_K \end{bmatrix} \tag{55}$$

Using Laplace decomposition, the determinant of $\mathbf{M}$ is

$$\det M = \left(a_0 - \sum_{n=1}^{N} \frac{a_n^2}{b_n}\right) \prod b_n \tag{56}$$

By using Cramer's rule and remarking that the minors of $\mathbf{M}$ have the same shape, the coefficients of the inverse of $M^{-1} = (m_{ij})_{0\le i,j\le K}$ are found as:

$$m_{00} = \frac{1}{a_0 - \sum_{k=1}^{K} \frac{a_k^2}{b_k}} \tag{57}$$

$$m_{0k} = m_{k0} = -\frac{a_k}{b_k} m_{00} \tag{58}$$

$$m_{kk} = \frac{1}{b_n} + \frac{a_k^2}{b_k^2} m_{00} \tag{59}$$

$$m_{ij} = \frac{a_i a_j}{b_i b_j} m_{00} \tag{60}$$

C. DOA estimation FIM

Using the model given by eq (3), and assuming a circular complex Gaussian white noise, the FIM $\mathbf{G}$ for the DOA estimation parameters with unknown frequency may be computed using the Slepian-Bangs formula.

Using the estimated parameters vector $[\beta_{1,1}, \alpha_{1,1}, \omega_1, \tau_{1,1}^{(0)}]$ (further noted $[\beta, \alpha, \omega, \tau]$), we can write :

$$\sigma^2\mathbf{G} = \begin{bmatrix} \sum_{k=1}^{K} N_k & 0 & 0 & 0 \\ 0 & G_{\alpha,\alpha} & G_{\alpha,\omega} & G_{\alpha,\tau} \\ 0 & G_{\alpha,\omega} & G_{\omega,\omega} & G_{\omega,\tau} \\ 0 & G_{\alpha,\tau} & G_{\omega,\tau} & \omega^2\beta^2 \sum_{k=1}^{K} N_k \end{bmatrix} \tag{61}$$

$$G_{\alpha,\alpha} = \omega^2\beta^2 \sum_{k=1}^{K} N_k \left(\frac{\partial \tau_k(\alpha)}{\partial \alpha}\right)^2 \tag{62}$$

$$G_{\omega,\omega} = \beta^2 \sum_{k=1}^{K} \sum_{n=1}^{N_k} \left(t_{k,n} - \tau_k(\alpha) - \tau^{(0)}\right)^2 \tag{63}$$

$$G_{\alpha,\tau} = \omega^2\beta^2 \sum_{k=1}^{K} N_k \frac{\partial \tau_k(\alpha)}{\partial \alpha} \tag{64}$$

$$G_{\alpha,\omega} = -\omega\beta^2 \sum_{k=1}^{K} \frac{\partial \tau_k(\alpha)}{\partial \alpha} \sum_{n=1}^{N_k} t_{k,n} - \tau_k(\alpha) - \tau^{(0)} \tag{65}$$

$$G_{\omega,\tau} = -\omega\beta^2 \sum_{k=1}^{K} \sum_{n=1}^{N_k} t_{k,n} - \tau_k(\alpha) - \tau^{(0)} \tag{66}$$

References

[1] H. Krim, M. Viberg, Two decades of array signal processing research: the parametric approach, IEEE Signal Processing Magazine 13 (4) (1996) 67–94. doi:10.1109/79.526899.

[2] B. G. Wahlberg, I. M. Y. Mareels, I. Webster, Experimental and theoretical comparison of some algorithms for beamforming in single receiver adaptive arrays, IEEE Transactions on Antennas and Propagation 39 (1) (1991) 21–28.

[3] Chong Meng Samson See, High resolution DF with a single channel receiver, in: Proceedings of the 11th IEEE Signal Processing Workshop on Statistical Signal Processing (Cat. No.01TH8563), 2001, pp. 520–523.

[4] J. Sheinvald, M. Wax, Direction finding with fewer receivers via time-varying preprocessing, IEEE Transactions on Signal Processing 47 (1) (1999) 2–9.

[5] C. . S. See, A single channel approach to high resolution direction finding and beamforming, in: 2003 IEEE International Conference on Acoustics, Speech, and Signal Processing, 2003. Proceedings. (ICASSP '03)., Vol. 5, 2003, pp. V–217.

[6] Z. Wang, W. Xie, Y. Zou, Q. Wan, DOA estimation using single or dual reception channels based on cyclostationarity, IEEE Access 7 (2019) 54787–54795. doi:10.1109/ACCESS.2019.2912907.

[7] D. N. Aloi, M. S. Sharawi, Comparative analysis of single-channel direction finding algorithms for automotive applications at 2400 MHz in a complex reflecting environment, Physical Communication 3 (1) (2010) 19 – 27.

[8] Moon-Sik Lee, V. Katkovnik, Yong-Hoon Kim, System modeling and signal processing for a switch antenna array radar, IEEE Transactions on Signal Processing 52 (6) (2004) 1513–1523.

[9] M.-S. Lee, V. Katkovnik, Y.-H. Kim, Robust approximate median beamforming for phased array radar with antenna switching, Signal Processing 84 (9) (2004) 1667 – 1675, special Section on New Trends and Findings in Antenna Array Processing for Radar. doi:https://doi.org/10.1016/j.sigpro.2004.05.007.
URL http://www.sciencedirect.com/science/article/pii/S0165168404000921

[10] M. Lee, Y. Kim, Design and performance of a 24-GHz switch-antenna array FMCW radar system for automotive applications, IEEE Transactions on Vehicular Technology 59 (5) (2010) 2290–2297.

[11] C. Hu, Y. Liu, H. Meng, X. Wang, Randomized switched antenna array FMCW radar for automotive applications, IEEE Transactions on Vehicular Technology 63 (8) (2014) 3624–3641.

[12] M. . Lee, V. Katovnik, Y. . Kim, Cramer-rao bound analysis for active array with antenna switching, Electronics Letters 39 (1) (2003) 7–8.

[13] E. A. Lee, J. Kim, H.-J. Kim, Y.-J. Chong, J. H. Cho, Calibration of a fully-switched MIMO channel sounder with internal crosstalk, Signal Processing 156 (2019) 21 – 30. doi:https://doi.org/10.1016/j.sigpro.2018.10.014.
URL http://www.sciencedirect.com/science/article/pii/S0165168418303463

[14] M. Cominelli, P. Patras, F. Gringoli, Dead on arrival: An empirical study of the bluetooth 5.1 positioning system, in: Proceedings of the 13th International Workshop on Wireless Network Testbeds, Experimental Evaluation & Characterization, WiNTECH '19, Association for Computing Machinery, New York, NY, USA, 2019, p. 13–20.

[15] Bluetooth Special Interest Group (SIG), Bluetooth Core Specification v5.1, Vol. 6.

[16] J. Sheinvald, M. Wax, Localization of multiple signals using subarrays data, in: 1995 International Conference on Acoustics, Speech, and Signal Processing, Vol. 3, 1995, pp. 2112–2115 vol.3. doi:10.1109/ICASSP.1995.478492.

[17] F. Wen, Q. Wan, R. Fan, H. Wei, Improved MUSIC algorithm for multiple noncoherent subarrays, IEEE Signal Processing Letters 21 (5) (2014) 527–530. doi:10.1109/{LSP}.2014.2308271.

[18] D. Slepian, Estimation of signal parameters in the presence of noise, Transactions of the IRE Professional Group on Information Theory 3 (3) (1954) 68–89. doi:10.1109/IREPGIT.1954.6373401.

[19] W. J. Bangs, Array processing with generalized beamformers, 1971.

[20] P. Stoica, R. L. Moses, Introduction to spectral analysis, Pearson Education, 1997.

[21] T. Routtenberg, J. Tabrikian, Cyclic barankin-type bounds for non-bayesian periodic parameter estimation, IEEE Transactions on Signal Processing 62 (13) (2014) 3321–3336. doi:10.1109/TSP.2014.2321117.

[22] A. Renaux, P. Forster, E. Chaumette, P. Larzabal, On the high-SNR conditional maximum-likelihood estimator full statistical characterization, IEEE Transactions on Signal Processing 54 (12) (2006) 4840–4843.

[23] E. W. Barankin, Locally best unbiased estimates, The Annals of Mathematical Statistics 20 (4) (1949) 477–501.
URL http://www.jstor.org/stable/2236306

[24] S. Samadian, R. Hayashi, A. A. Abidi, Demodulators for a zero-IF bluetooth receiver, IEEE Journal of Solid-State Circuits 38 (8) (2003) 1393–1396. doi:10.1109/JSSC.2003.814419.

[25] M. Silva Pereira, J. Caldinhas Vaz, C. Azeredo Leme, J. T. de Sousa, J. Costa Freire, A 170 μA all-digital GFSK demodulator with rejection of low SNR packets for bluetooth-LE, IEEE Microwave and Wireless Components Letters 26 (6) (2016) 452–454. doi:10.1109/LMWC.2016.2562639.

[26] F. Pukelsheim, Optimal Design of Experiments, Society for Industrial and Applied Mathematics, 2006. doi:10.1137/1.9780898719109.